ELSEVIER

Journal of Hydrology 159 (1994) 145–167

Journal of Hydrology

[3]

Dispersion at the field scale resulting from spatial variability of the hydraulic conductivity field

L. Boersma*[,a], F.T. Lindstrom[b], M.A. Barlaz[c]

[a]*Department of Crop and Soil Science, Oregon State University, Corvallis, OR 97331-7306, USA*
[b]*Reynolds Electrical and Engineering Co., Inc., P.O. Box 98521, Las Vegas, NV 89193-8521, USA*
[c]*Department of Civil Engineering, North Carolina State University, Raleigh, NC 27695-7908, USA*

(Received 6 April 1992; revision accepted 29 June 1993)

Abstract

A two-dimensional mathematical model for simulating the transport and fate of chemicals in aquifers with spatially heterogeneous but isotropic fluid flow properties was developed, as part of an evaluation of bioremediation technologies that include injection of reactants into the aquifer. An important physical process is dispersion of the injected reactant in the aquifer. Dispersion was simulated with the model which has user-prescribed hydraulic pressure fields at the inflow and outflow boundaries. The model accounts for the major physical processes of dispersion and advection and several fundamental chemical and biological processes, including linear equilibrium sorption, irreversible sorption and/or dissolution into an organic phase, microbial degradation, radioactive decay, and other irreversible processes. The chemical may be released internally via distributed leaks from sources that do not perturb the flow field, from fully penetrating injection wells, or it may enter at the inlet boundary. The chemical transport and fate equations are solved in terms of user-stipulated initial and boundary conditions.

Simulations were made to evaluate dispersion resulting from spatial variability in the hydraulic conductivity (K). Flow fields were divided into regions with hydraulic conductivities of 0.2, 2.0 and 20 m day^{-1}. Distributions of chemical, initially present as a distributed source near the inflow boundary, were obtained for several geometries of the hydraulic conductivity regions. Results show the influence on distributions of regions of low, medium, and high K; they demonstrate the importance of knowledge about the hydraulic conductivity field, both for interpretation of sampling data and for prediction of plume behaviour in terms of direction of movement, dispersion and rate of travel.

* Corresponding author.

0022-1694/94/$07.00 © 1994 – Elsevier Science B.V. All rights reserved
SSDI 0022-1694(94)05066-7

1. Introduction

Aquifer pollution is a rapidly growing problem in the United States (Pye et al., 1983) and other countries. The true extent of groundwater contamination is not known because measurements of the problem have only recently been made on a consistent basis.

Various methods have been used to restore the quality of groundwater. Two major categories are physical containment and chemical and/or biological treatment (Lehr and Nielsen, 1982). Physical methods, including the placement of barriers or hydrodynamic control by pumping, have been used with some success but these methods are most effective when used to isolate point sources of pollution rather than to restore water quality in aquifers. Removal of pollutants from the groundwater is a more reasonable strategy for pollutants contributed by non-point sources or by widely distributed sources. Chemical and biological methods are commonly used in situations where water is pumped out, treated, and used (e.g. Van der Hoek and Klapwijk, 1987). This class of methods is used extensively for drinking water supplies where the end product is important enough to justify the expense.

A significant advantage of chemical and biological methods is the possibility of in situ aquifer restoration. Various chemical techniques have been used for this purpose (Brown et al., 1985). There is also considerable interest in the rapidly growing field of biorestoration (Alexander, 1981; Lehr and Nielsen, 1982; Brown et al., 1985; Lee et al., 1988). The challenge of in situ methods is the maintenance of appropriate conditions for stimulation of biological activity in the aquifer. For biorestoration, the important factors affecting the rate and efficiency of contaminant biodegradation are the presence of microbes suitable for metabolizing the pollutants, the presence of energy sources and electron acceptors to sustain adequate microbial growth, the distribution of pollutant, substrate, and organisms in the aquifer, and flow properties of the aquifer, including hydraulic gradients, spatial variation in hydraulic conductivity and in physical and chemical properties of the aquifer material. The spreading of solutes is of most concern, because it determines the outline of the contaminant plume and impacts on decisions regarding placement of sampling wells and placement of wells for the injection of reactants for stimulation of reclamation.

Analysis of solute transport is based on the advection–dispersion equation where the advective part describes the transport at the mean velocity and the dispersive part describes the spreading of solutes in the medium caused by hydrodynamic dispersion and molecular diffusion. Hydrodynamic dispersion refers to the distribution or spreading of solute resulting from the range of velocities which exists in individual pore channels (Hillel, 1980). On a larger scale, i.e. field scale, hydrodynamic dispersion occurs as a result of changes in hydraulic conductivity in the flow field owing to heterogeneity of the aquifer material. The form of spreading resulting from these changes in the hydraulic conductivity, usually referred to as macro-scale dispersion, is the focus of this paper.

The advection–dispersion equation introduces the dispersivity tensor as a measure of dispersion. Determination of the value of dispersivity has been the subject of many studies which have led to the general agreement that laboratory experiments cannot

be expected to yield values of dispersivity applicable to field conditions (Dagan, 1984; Gelhar, 1986; Hess et al., 1992). Since dispersion at the field scale is governed by spatial variability in hydraulic conductivity, the traditional approach has been to base calculation of the macrodispersivity tensor on a statistical analysis of the hydraulic conductivity. Knowledge of the statistical properties of the spatial distribution of K, namely variance and correlation scales, yields values which can be used in stochastic transport theories. Hess et al. (1992) reviewed and summarized recent studies, and concluded that this approach shows good agreement between predicted and measured distributions. Clearly, the statistical approach has made rapid advances possible. Nevertheless, additional insights can be gained by an evaluation of the manner in which placement, shape and size of regions of different hydraulic conductivities interact. Understanding this interaction is particularly important in decisions regarding placement of wells for injecting reactant intended to stimulate bioremediation.

To gain further insights into the impact of macrodispersion on contaminant transport, an approach was developed based on mathematical modelling techniques such as are used to good effect in the analysis of problems of contaminated aquifers. The development of models is often a cost-effective method of deciding between alternative remediation scenarios for a given problem. This is particularly true for biological remediation where the outcome of treatments is often uncertain.

The model developed for the analysis of macrodispersion is based on a two-dimensional, horizontal, steady-state, fluid flow field defined by a hydraulic head field which is dependent upon appropriate Dirichlet and Neumann boundary conditions and characterization of the spatial dependency of the saturated hydraulic conductivity. The model accounts for two-dimensional transport and the fate of chemicals in a non-homogeneous aquifer. The distribution of chemicals is affected by advection and dispersion in both the longitudinal and transverse directions, by linear equilibrium adsorption/desorption processes, by first-order loss processes, including metabolism by soil microbes or chemical reactions with other soil components in the free and/or sorbed phases, or by other irreversible processes which may operate in either the free or sorbed phases. The model allows the presence of zero-order sources of chemical, appropriate Dirichlet and Neumann boundary conditions with a provision for non-zero initial distribution of the chemical, and the presence of fully penetrating injection and/or extraction wells.

It is assumed that the chemical and biological process coefficients are at least piecewise differentiable functions of the transverse coordinate, x, and of the longitudinal coordinate, y. The mathematical symbols used in this manuscript and their physical or chemical meaning are stated in the text when they are first introduced.

The simulations conducted with the model were to determine the distribution of chemical, initially present in a source area near the inflow boundary, for several scenarios of spatial variability of hydraulic conductivity. Flow fields were divided into regions with hydraulic conductivities ranging from 0.2 to 20.0 m day^{-1}. Plume development was evaluated during 150 days of simulated transport for each geometry of the hydraulic conductivity regions.

2. Mathematical model

2.1. Statement of the problem

The mathematical model pertains to an aquifer made up of a single layer with water entering and leaving an inflow and outflow boundary defined by a constant head, H (m) (Fig. 1). The model was developed for applications that include injection and extraction wells for in situ chemical and/or biorestorations. Thus, water can be extracted or injected through arbitrarily placed fully penetrating injection and/or extraction wells. The porous medium may be non-homogeneous and anisotropic. The assumptions concerning the fluid flow field are that:

(1) the fluid flow field operates at steady-state conditions at all times;

(2) any fluid flow perturbations introduced at either of the flow boundaries propagate extremely rapidly throughout the flow field, so that a new steady state is achieved instantaneously and the fluid storativity term in the fluid flow model may be neglected (Bodvarsson, 1984);

(3) the aquifer material is isotropic, but may be heterogeneous;

(4) the hydraulic conductivity function is differentiable almost everywhere;

(5) Dirichlet boundary conditions hold at both the inflow and outflow boundaries;

(6) inflow hydraulic head (H_{in}) and outflow hydraulic head (H_{out}) are specified and extend across the length of the boundary ($0 \leq x \leq L_x$) (Eqs. 4 and 5);

(7) Neumann no-flux-type boundary conditions are specified along the longitudinal boundaries, i.e. the $x = 0$ and $x = L_x$ planes (Eqs. 6 and 7).

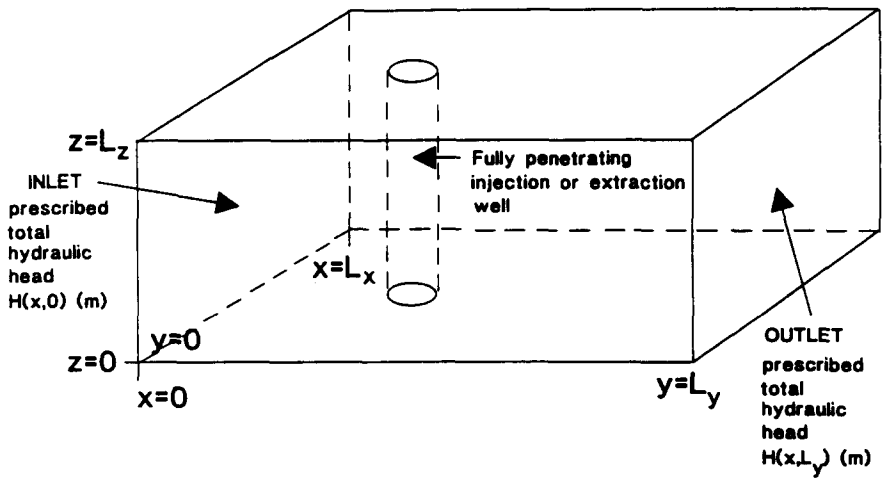

Fig. 1. Schematic diagram of the conditions for which the computer model was developed. The mathematical model allows for the arbitrary placement of injection and/or extraction wells. These were not included in the discussion in this paper.

2.2. Fluid flow field

The velocity field components of the flow vector $\boldsymbol{q}$ are defined by

$$\boldsymbol{q} = (\epsilon U_x, \epsilon U_y) = \left(-K_{sxx}\frac{\partial H}{\partial x}, -K_{syy}\frac{\partial H}{\partial y}\right) \tag{1}$$

where $\boldsymbol{q}$ is the Darcy velocity vector ($m\,day^{-1}$), ϵ is the porosity ($m^3\,m^{-3}$), U_x and U_y are the x and y components of the average seepage velocity ($m\,day^{-1}$), K_{sxx} and K_{syy} are transverse and longitudinal components of the saturated hydraulic conductivity in the aquifer ($m\,day^{-1}$) and H is the hydraulic head (m). The coordinate system is chosen to coincide with the two principal directions of flow (Bear and Verruijt, 1987, p. 39). The steady-state continuity equation for a representative elementary volume (REV) in the aquifer is given by

$$\nabla \cdot (\rho_w \boldsymbol{q}) = (Q_{inj} - Q_{out}) \tag{2}$$

where ρ_w is the density of water ($kg\,m^{-3}$) which is assumed constant, Q_{inj} is the fluid mass injection rate ($kg\,m^{-3}\,day^{-1}$) and Q_{out} is the fluid mass extraction rate ($kg\,m^{-3}\,day^{-1}$). Substitution for $\boldsymbol{q}$ in Eq. (2) yields the Poisson equation

$$\rho_w\left[\frac{\partial\left(-K_{sxx}\frac{\partial H}{\partial x}\right)}{\partial x} + \frac{\partial\left(-K_{syy}\frac{\partial H}{\partial y}\right)}{\partial y}\right] = \rho_w\left[\frac{\partial(\epsilon U_x)}{\partial x} + \frac{\partial(\epsilon U_y)}{\partial y}\right] = (Q_{inj} - Q_{out}) \tag{3}$$

K_{sxx}, K_{syy}, and ϵ are assumed to be almost everywhere differentiable functions of x and y inside the flow domain.

Boundary conditions, to be satisfied at all times, are written according to assumptions (5) and (6) as follows:
along $y = 0$ (inlet end),

$$H(x,0) = H_{in}(x), 0 \le x \le L_x \tag{4}$$

along $y = L_y$ (outlet end),

$$H(x,L_y) = H_{out}(x), 0 \le x \le L_x \tag{5}$$

along $x = 0$,

$$\frac{\partial H}{\partial x} = 0 \tag{6}$$

along $x = L_x$,

$$\frac{\partial H}{\partial x} = 0 \tag{7}$$

K_{sxx} and K_{syy} may vary by several orders of magnitude over the interior of the flow

domain. An analytical solution of Eq. (3), subject to boundary conditions Eqs. (4)–(7), where K_{sxx} and K_{syy} are variable, does not appear to be obtainable. Lindstrom and Boersma (1989) gave an analytical representation of the problem for an isotropic medium in which $K_{sxx} = K_{syy} = K_s$ is constant, in terms of a double sum infinite series of trigonometric functions, i.e. a classical eigenfunction solution procedure. However, even in the very special case of constant K_{sxx} and K_{syy}, the solutions are usually very slow to converge. A very large number of terms is necessary to achieve the required number of significant digits in each velocity component. Thus, the hydraulic head field on the interior of the aquifer will be approximated via space–centred finite difference, or finite element methods.

2.3. Transport and fate equations

The assumptions that form the basis for the chemical transport and fate model are that:

(1) mass transport is via advection (convection) and dispersion;

(2) the x and y dispersion components are linearly dependent upon the moduli of the fluid velocity field components;

(3) the porous medium can be partitioned into three classes with respect to sorption, namely, weakly sorbing particles, sorbing particles (clay or small silt particles), and a strongly sorbing organic fraction for which linear equilibrium sorption rules are assumed to hold as follows

$$S = [(M_{ws}/M_t)\rho_{ws}K_{ws} + (M_s/M_t)\rho_s K_s + (M_o/M_t)\rho_o K_o]C \tag{8}$$

where the subscripts ws, s, o, and t denote non-sorbing, sorbing, strongly sorbing and total fractions of the aquifer materials, M is mass of materials, ρ is the average particle density, and K is the linear equilibrium distribution coefficient;

(4) chemical can be introduced into the aquifer with the inflow stream at the inlet end ($y = 0$) or from constantly emitting sources in the aquifer;

(5) density gradients, density stratifications, or local changes in the transport and/or fate properties of the porous medium are negligible;

(6) water containing dissolved chemicals can be introduced via fully penetrating injection wells and/or extracted from similar wells by pumping;

(7) loss of chemical can occur via first-order loss processes including microbial and/or chemical irreversible processes in both the free and sorbed phases;

(8) all first-order loss process coefficients are continuous functions of x and y inside the aquifer.

The second assumption, namely that the x and y dispersion components are linearly dependent upon the moduli of the velocity field components implies that for two-dimensional flow in an isotropic and non-homogeneous aquifer (Bear and Verruijt, 1987, pp. 161–164),

$$D_{xx} = \alpha_{tort}D_{L0} + \alpha_{dispx}\frac{(U_x)^2}{|U|} + \alpha_{dispy}\frac{(U_y)^2}{|U|} \tag{9}$$

and

$$D_{yy} = \alpha_{\text{tort}} D_{\text{L0}} + \alpha_{\text{dispx}} \frac{(U_x)^2}{|U|} + \alpha_{\text{dispy}} \frac{(U_y)^2}{|U|} \tag{10}$$

where the magnitude of the local seepage velocity vector U is defined by

$$|U| = [(U_x)^2 + (U_y)^2]^{1/2} \tag{11}$$

and the 'longitudinal' axis coincides with the y-axis (Konikow and Bredehoeft, 1978). D_{xx} and D_{yy} are the dispersion coefficients in the x and y directions, α_{tort} is tortuosity and α_{dispx} and α_{dispy} are dispersivities. The cross-axis dispersion coefficient D_{xy} is symmetrical so that $D_{yx} = D_{xy}$ and

$$D_{xy} = (\alpha_{\text{dispy}} - \alpha_{\text{dispx}}) \frac{U_x U_y}{|U|} \tag{12}$$

The longitudinal and transverse dispersivities ($\alpha_{\text{dispy}}, \alpha_{\text{dispx}}$) as well as the tortuosity (α_{tort}) are assumed to be piecewise differentiable functions of x and y inside the flow domain.

Consideration of the balance of chemical mass in the representative elementary volume (REV) leads to the linear two-dimensional transport and fate equation:

$$\begin{aligned} \epsilon(1+R)\frac{\partial C}{\partial t} = {} & \frac{\partial}{\partial x}\left(\epsilon D_{xx}\frac{\partial C}{\partial x}\right) + \frac{\partial}{\partial y}\left(\epsilon D_{yy}\frac{\partial C}{\partial y}\right) \\ & + \frac{\partial}{\partial x}\left(\epsilon D_{yy}\frac{\partial C}{\partial y}\right) + \frac{\partial}{\partial y}\left(\epsilon D_{yx}\frac{\partial C}{\partial x}\right) \\ & - \frac{\partial}{\partial x}(\epsilon U_x C) - \frac{\partial}{\partial y}(\epsilon U_y C) \\ & - \epsilon[\lambda_{\text{met}} + \lambda_{\text{irr}} + \lambda_{\text{rad}} + R(\lambda^{\text{s}}_{\text{met}} + \lambda^{\text{s}}_{\text{rad}})]C + Q_{\text{so}} \\ & + Q_{\text{inj}} C_{\text{s}} - \frac{Q_{\text{out}}}{\rho_{\text{w}}} C \end{aligned} \tag{13}$$

with

$$R = \frac{(1-\epsilon)}{\epsilon}[(M_{\text{ws}}\rho_{\text{ws}}K_{\text{ws}} + M_{\text{s}}\rho_{\text{s}}K_{\text{s}} + M_{\text{s}}\rho_{\text{o}}K_{\text{o}})]/M_{\text{t}} \tag{14}$$

R is usually called the retention coefficient (dimensionless) in gas chromatography literature, but in the soil science literature the retardation coefficient $R_{\text{d}} = 1 + R$ is mostly used. Defining the overall first-order loss coefficient Λ (day^{-1}) by

$$\Lambda = \lambda_{\text{met}} + \lambda_{\text{irr}} + \lambda_{\text{rad}} + R(\lambda^{\text{s}}_{\text{met}} + \lambda^{\text{s}}_{\text{rad}}) \tag{15}$$

where the λ's are first-order loss rate constants in the free phase for irreversible loss owing to metabolic processes (λ_{met}), loss owing to radioactive decay (λ_{rad}), and loss owing to other irreversible processes (λ_{irr}), e.g. chemical reactions and superscript s

refers to the sorbed phase. Substituting Eq. (3) into Eq. (13) yields

$$\begin{aligned}\epsilon(1+R)\frac{\partial C}{\partial t} = &\frac{\partial}{\partial x}\left(\epsilon D_{xx}\frac{\partial C}{\partial x}\right)+\frac{\partial}{\partial x}\left(\epsilon D_{xy}\frac{\partial C}{\partial y}\right)\\ &+\frac{\partial}{\partial y}\left(\epsilon D_{yy}\frac{\partial C}{\partial y}\right)+\frac{\partial}{\partial y}\left(\epsilon D_{yx}\frac{\partial C}{\partial x}\right)\\ &-(\epsilon U_x)\frac{\partial C}{\partial x}-(\epsilon U_y)\frac{\partial C}{\partial y}-\epsilon\Lambda C+Q_{so}\\ &+Q_{inj}(C_s-C/\rho_w)\end{aligned} \tag{16}$$

Even though Eq. (16) is linear and the aquifer is a rectangular domain, the fact that U_x, U_y, D_{xx}, D_{yy} and D_{xy} can all vary quite widely over this domain has made it impossible to obtain closed-form solutions except for the case of constant coefficients with $\alpha_{dispx} = \alpha_{dispy}$. Such conditions rarely occur at the field scale which has made it necessary to solve Eq. (16) for $C(x, y, t)$ approximately. The finite-difference Euler–Lagrange procedure (Cheng et al., 1984) which is a modification of the method of characteristics, was chosen as the basis for developing a solution to Eq. (16).

2.4. Method of solution

In anticipation of the Euler–Lagrange solution procedure, the advection terms were brought to the left-hand side of Eq. (16) and the expression was multiplied by the factor $1/[\epsilon(1+R)]$ to obtain

$$\begin{aligned}&\frac{dC}{dt}+U_x^*\frac{\partial C}{\partial x}+U_y^*\frac{\partial C}{\partial y}+\Lambda^* C\\ &\quad=\left[\frac{\partial}{\partial x}\left(\epsilon D_{xx}\frac{\partial C}{\partial x}\right)+\frac{\partial}{\partial y}\left(\epsilon D_{yy}\frac{\partial C}{\partial y}\right)+\frac{\partial}{\partial y}\left(\epsilon D_{yx}\frac{\partial C}{\partial x}\right)\right.\\ &\quad\left.+\frac{\partial}{\partial x}\left(\epsilon D_{xy}\frac{\partial C}{\partial y}\right)\right]/[\epsilon(1+R)]+\frac{Q_{so}^*}{\epsilon}+\frac{Q_{inj}^*}{\epsilon}(C_s-C/\rho_w)\end{aligned} \tag{17}$$

where the 'effective' transport and fate coefficients are defined

$$U_x^* = \frac{U_x}{1+R}, \qquad U_y^* = \frac{U_y}{1+R}, \qquad \text{and } \Lambda^* = \frac{\Lambda}{1+R} \tag{18}$$

and the 'effective' source/sink mass rates are defined by

$$Q_{so}^* = \frac{Q_{so}}{1+R} \tag{19}$$

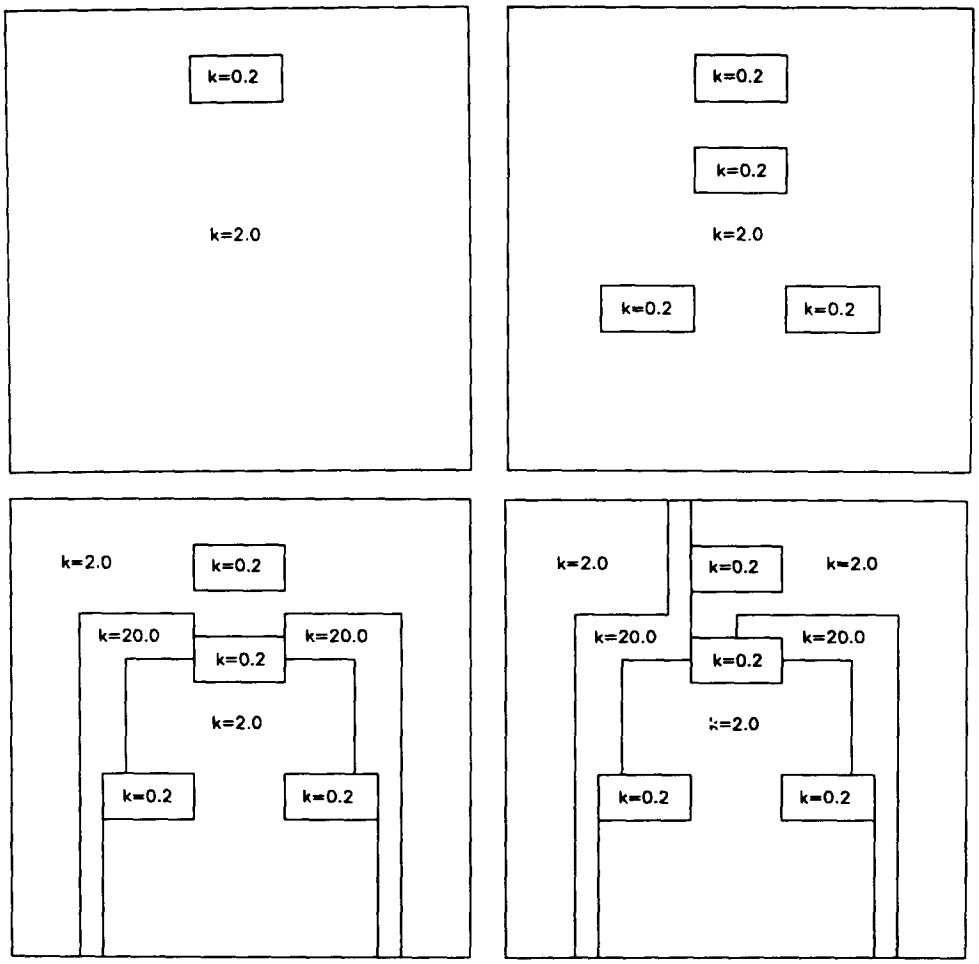

Fig. 2. Hydraulic conductivity fields for several of the scenarios evaluated in the manuscript. Flow is from the top to the bottom for all simulations shown. A non-sorbing chemical with $D = 1.43 \times 10^{-4}\ \mathrm{m^2\,day^{-1}}$ was assumed to be initially present in the region of low hydraulic conductivity near the inflow end. Evaluation of dispersion owing to geometry of hydraulic conductivity areas was based on the distribution of the chemical at the end of 50, 100 and 150 days of simulated transport.

and

$$Q^*_{\mathrm{inj}} = \frac{Q_{\mathrm{inj}}}{1+R} \tag{20}$$

Since the 'effective' material or total derivative $\mathrm{d}C/\mathrm{d}t$ is

$$\frac{\mathrm{d}C}{\mathrm{d}t} = \frac{\partial C}{\partial t} + U^*_x \frac{\partial C}{\partial x} + U^*_y \frac{\partial C}{\partial y} \tag{21}$$

Table 1
Values of parameters used in simulations with LT2VSI

Parameter	Symbol	Value	Units
		low/medium/high	
Porosity	ϵ	0.465/0.365/0.285	$m^3\ m^{-3}$
Tortuosity	α_{tort}	0.50/0.67/0.90	
Non-sorbing mass fraction	M_{ws}/M_t	0.8/0.95/1.0	
Sorbing mass fraction	M_s/M_t	0.19/0.05/0.0	
Strongly sorbing mass fraction	M_o/M_t	0.01/0.0/0.0	
Pressure head, inflow boundary	H_{in}	10.0	m water
Pressure head, outflow boundary	H_{out}	0.0	m water
Dispersivity, x component	α_{dispx}	1.0E-2/3.5E-3/1.2E-3	m
Dispersivity, y component	α_{dispy}	1.0E-2/3.5E-3/1.2E-3	m
Hydraulic conductivity	$K_{xx} = K_{yy}$	0.2/2.0/20.0	$m\ day^{-1}$
Initial chemical concentration	C	1.0/0.0/0.0	$kg\,m^{-3}$
Diffusion coefficient		0.000143	$m^2\ day^{-1}$

Areas of low, medium and high conductivities are defined in text.

then

$$\frac{dC}{dt} + \Lambda^* C = \left[\frac{\partial}{\partial x}\left(\epsilon D_{xx}\frac{\partial C}{\partial x}\right) + \frac{\partial}{\partial y}\left(\epsilon D_{yy}\frac{\partial C}{\partial y}\right) + \frac{\partial}{\partial x}\left(\epsilon D_{xy}\frac{\partial C}{\partial y}\right) + \frac{\partial}{\partial y}\left(\epsilon D_{yx}\frac{\partial C}{\partial x}\right)\right] / [\epsilon(1+R)] + \frac{Q^*_{so}}{\epsilon} + \frac{Q^*_{inj}}{\epsilon}(C_s - C/\rho_w) \tag{22}$$

for the transport and fate equation. Boundary conditions, initial conditions and methods of solution were set forth in detail by Lindstrom et al. (1990, 1991). The model was referred to as LT2VSI.

3. Simulations

The model LT2VSI was developed for the evaluation of bioremediation scenarios for aquifers polluted with nitrate. The suggestion has been made that nitrates can be eliminated from groundwater through the addition of a carbon source to enhance conversion of nitrate to nitrogen gas by microorganisms. In this bioremediation concept the substrate would be added to the existing groundwater stream through injection wells.

To achieve maximum benefits of the injected substrates, maximum dispersion in the aquifer must be achieved. As dispersion increases, the number of wells required for

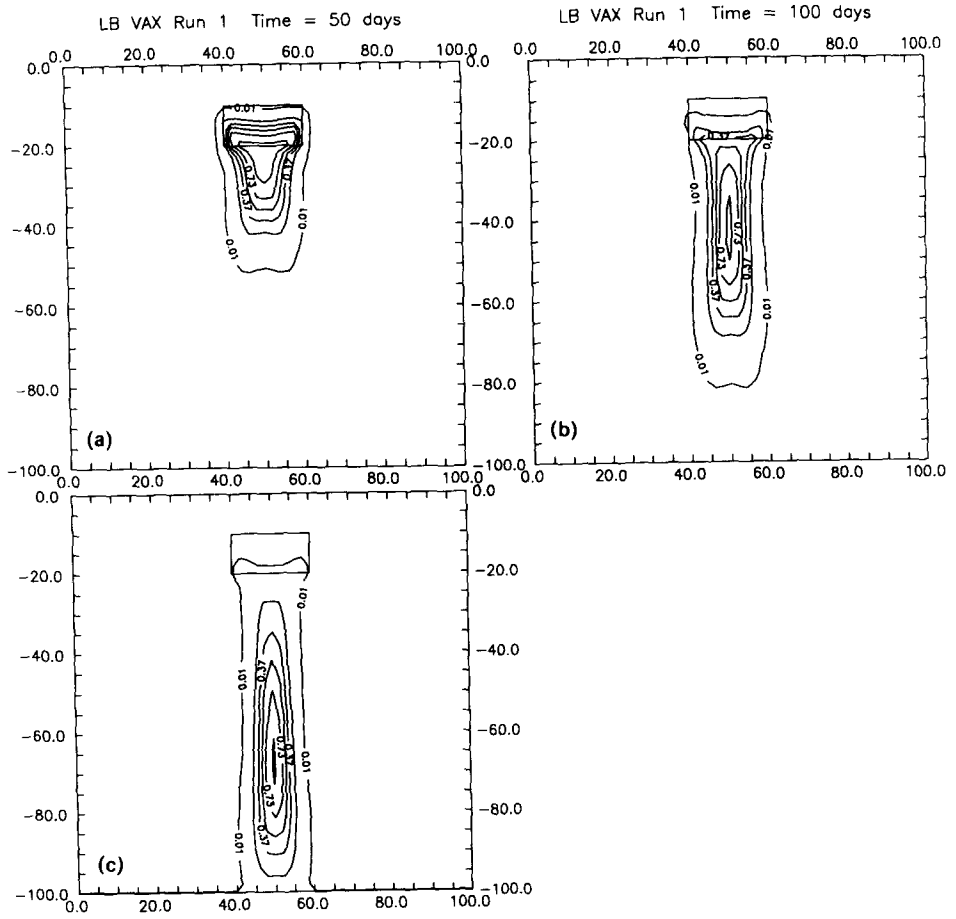

Fig. 3. Simulation 1. Distribution of the non-sorbing chemical, initially present in the source area defined by (40, 10; 60, 10; 60, 20; 40, 20), after 50, 100 and 150 days of simulated transport, shown in frames labelled (a), (b) and (c), respectively. Hydraulic conductivity $K = 2.0\,\mathrm{m\,day^{-1}}$ throughout, except in source area where $K = 0.2\,\mathrm{m\,day^{-1}}$.

complete coverage of the contaminated area decreases. Experience with several field-scale dispersion experiments suggests that dispersion resulting from spatial variability in the hydraulic conductivity field is often unpredictable.

To evaluate dispersion induced by spatial variability of the hydraulic conductivity field, several scenarios were postulated for which simulations, using LT2VSI, were carried out. Some of these, but not all of them, are shown in Fig. 2. A non-sorbing chemical with diffusion coefficient $D = 1.43 \times 10^{-4}\,\mathrm{m^2\,day^{-1}}$ was assumed to be present initially in a region of low hydraulic conductivity ($0.2\,\mathrm{m\,day^{-1}}$) near the inflow end of an area of dimensions $100 \times 100\,\mathrm{m^2}$. The hydraulic conductivity of the aquifer was set at $2.0\,\mathrm{m\,day^{-1}}$ and regions of low ($0.2\,\mathrm{m\,day^{-1}}$) and high ($20.0\,\mathrm{m\,day^{-1}}$) hydraulic conductivity were assumed to exist as indicated for each scenario. Data that were used for the scenarios are presented in Table 1. Evaluation of

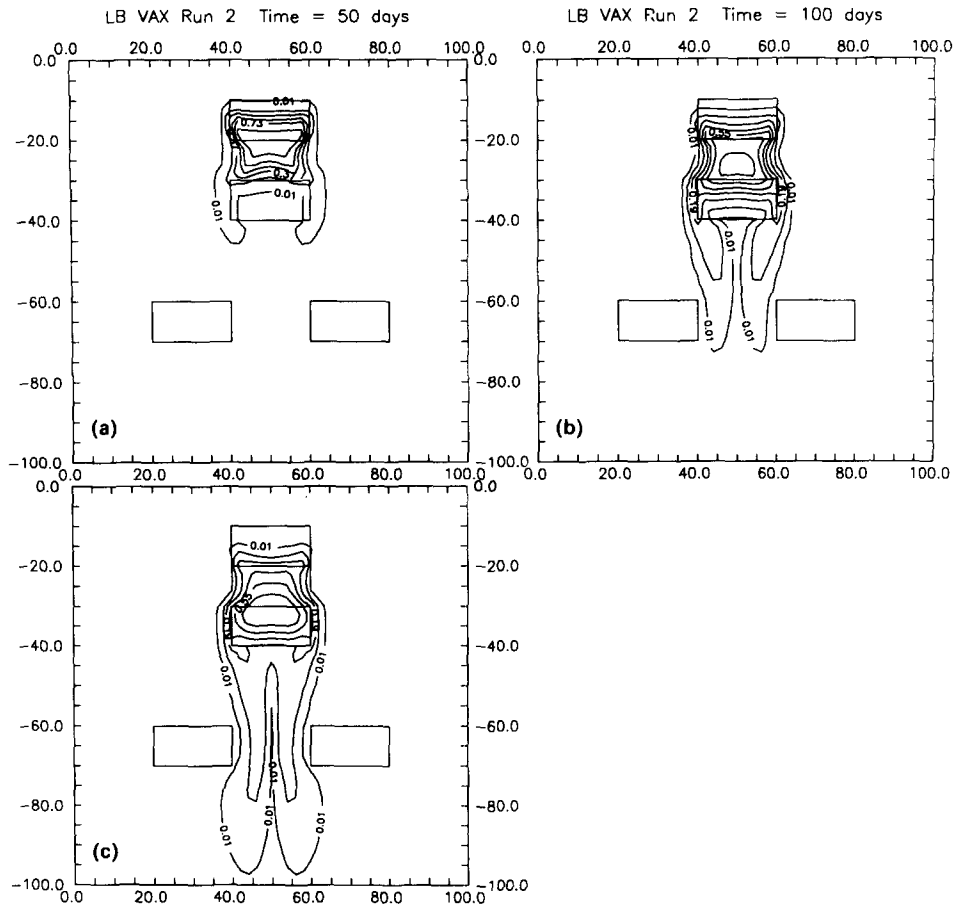

Fig. 4. Simulation 2. Distribution of the non-sorbing chemical, initially present in the source area defined by (40, 10; 60, 10; 60, 20; 40, 20), after 50, 100 and 150 days of simulated transport, shown in frames labelled (a), (b) and (c), respectively. Hydraulic conductivities were the same as in Fig. 2, with three regions with hydraulic conductivity $K = 0.2\,\mathrm{m\,day^{-1}}$ added as shown.

dispersion was based on the distributions of the chemical at the end of 50, 100, and 150 days of simulation. Fig. 3 (simulation 1) shows the distribution for an aquifer with $K = 2.0\,\mathrm{m\ day^{-1}}$ everywhere except in the source area, where $K = 0.2\,\mathrm{m\ day^{-1}}$. These distributions were compared with distributions for scenarios with regions of either lower or higher hydraulic conductivity in the aquifer as shown in Fig. 2. These geometries are repeated in the diagrams showing the results of the simulations (Figs. 3–12).

The dispersivities α_{dispx} and α_{dispy} were set equal to each other (Table 1). This assumption was dictated by the objectives of the exercise, namely, to demonstrate the shapes of plumes, i.e. macrodispersion caused by a priori known variability in the hydraulic conductivity field. With the simulations, the spatial variability of hydraulic conductivity is known and macrodispersion is revealed by numerical solutions of the

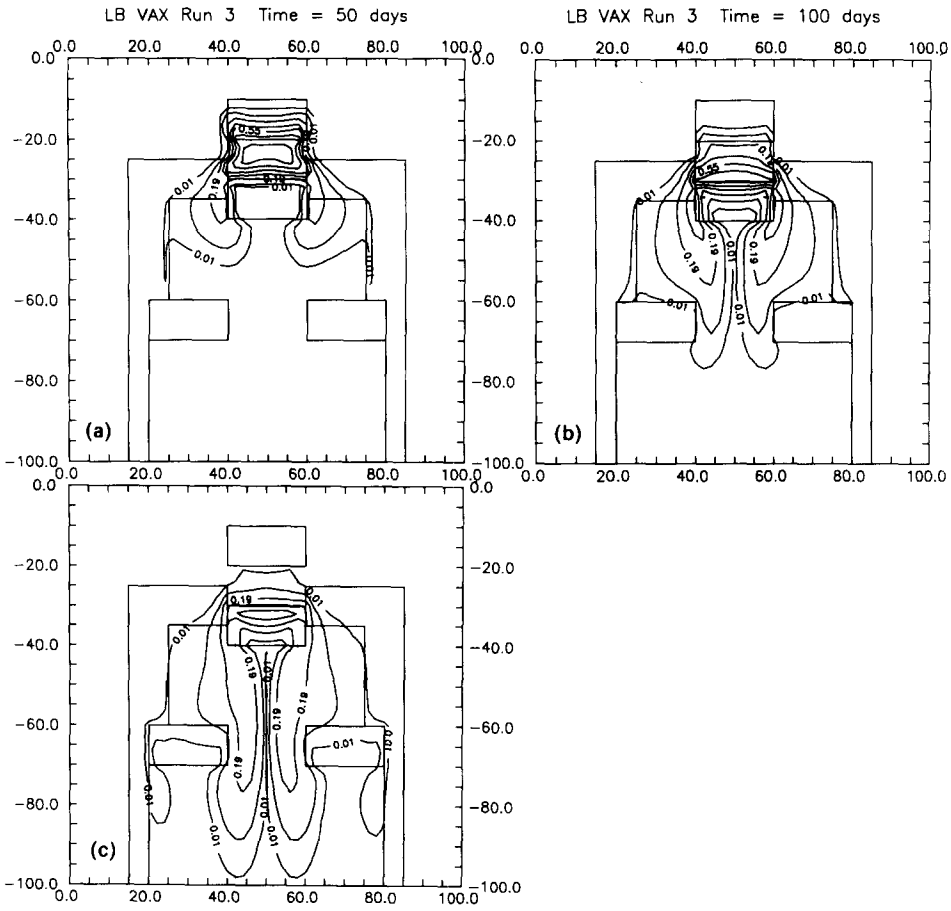

Fig. 5. Simulation 3. Distribution of the non-sorbing chemical, initially present in the source area defined by (40, 10; 60, 10; 60, 20; 40, 20), after 50, 100 and 150 days of simulated transport, shown in frames labelled (a), (b) and (c), respectively. Conditions were the same as with simulation 2, with two regions with high conductivity ($K = 20.0\,\mathrm{m\,day^{-1}}$) added.

advection–dispersion equation. One reason for demonstrating the results is to call attention to the fact that complicated and unexpected dispersion patterns may result from simple geometries of hydraulic variability fields. These results indicate why it may be difficult to develop a well-defined relationship between dispersity and properties of the aquifer. The shape and position of the plume were determined by the distribution of hydraulic conductivity in the aquifer and the release of the non-sorbing chemical from the source area with $K = 0.2\,\mathrm{m\,day^{-1}}$.

Spacing of the nodes has a large effect on the shape and concentration of the distributions computed. This effect will be considered later in the discussion. Simulations 1–6 (Figs. 3–8) were run with a nodal spacing of 1 m throughout the aquifer with additional nodes at 0.1 m on each side of boundaries of conductivity regions and along flow field boundaries.

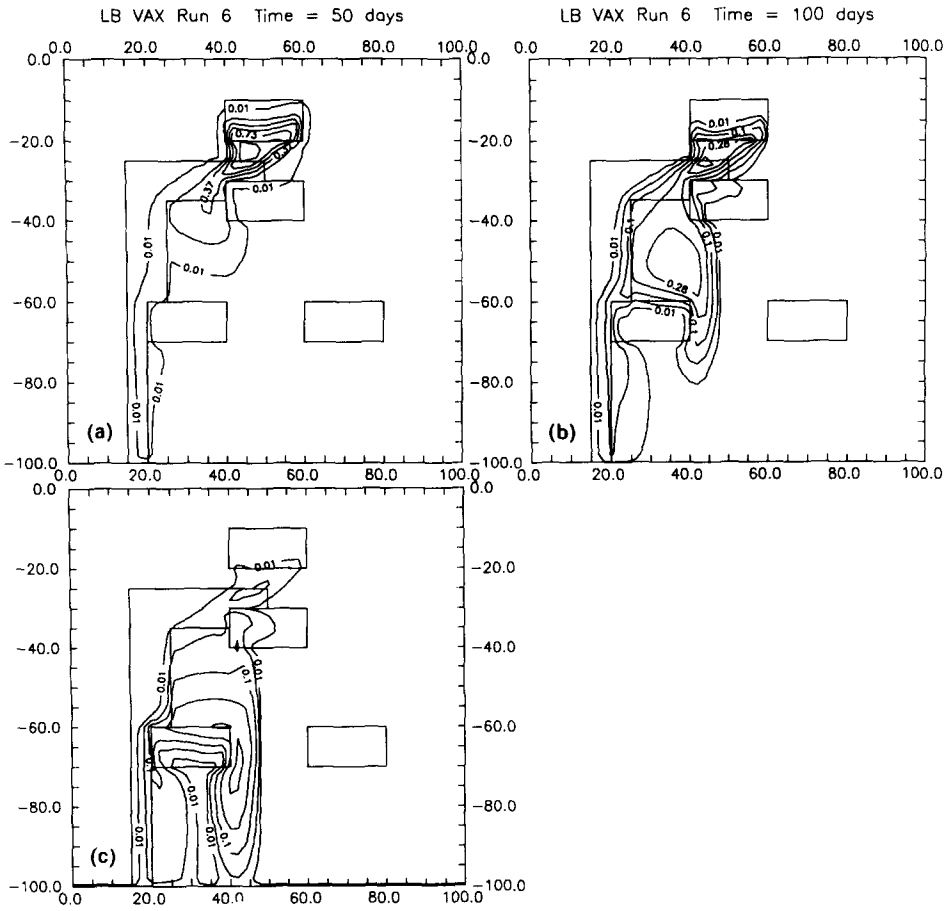

Fig. 6. Simulation 4. Distribution of the non-sorbing chemical, initially present in the source area defined by (40, 10; 60, 10; 60, 20; 40, 20), after 50, 100 and 150 days of simulated transport, shown in frames labelled (a), (b) and (c), respectively. Conditions were the same as with simulation 3 with one region with high conductivity omitted.

As a first step in increasing the complexity of the hydraulic conductivity field three areas of low conductivity (0.2 m day^{-1}) were added as shown in Fig. 4. Changes in the distributions from simulation 1 (Fig. 3 vs. Fig. 4) followed from the presence of the low-conductivity areas. The low-conductivity region immediately below the initial distribution forced flow in the lateral direction and retarded flow as well so that the plume did not advance as far downstream as occurred with scenario 1 during the 150 days of simulation. The presence of the two regions of low conductivity further downstream created a region of increased velocity between them, so that the water with the non-sorbing chemical passed there. The centre of mass of the plume did not advance as far as with simulation 1 and the leading edge concentration was more dilute, as indicated by lines of equal concentration.

For simulation 3 (Fig. 5), two regions of high conductivity (20.0 m day^{-1}) were

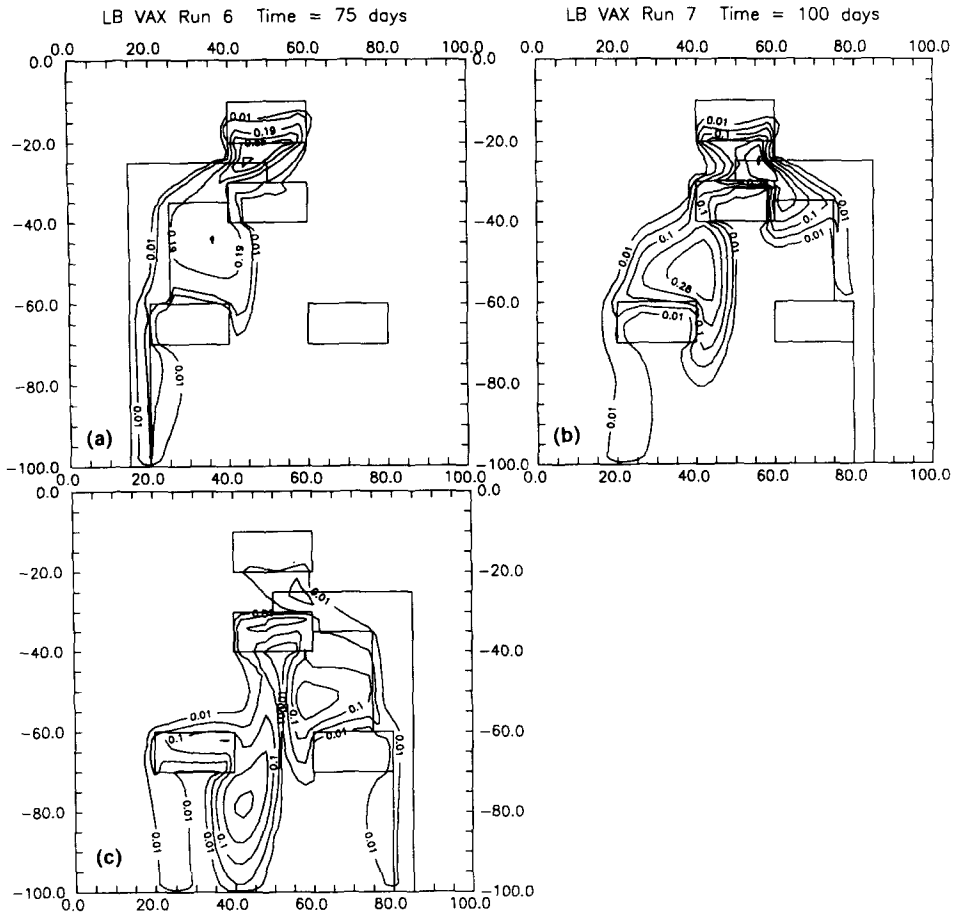

Fig. 7. Simulation 5. Distribution of non-sorbing chemical, initially present in the source area defined by (40, 10; 60, 10; 60, 20; 40, 20), after 50, 100 and 150 days of simulated transport, shown in frames labelled (a), (b) and (c), respectively. Conditions were the same as with simulation 4 during the first 75 days of simulation. After 75 days the path with $K = 20\,\mathrm{m\ day^{-1}}$ was changed from one side of the aquifer to the other.

added to the flow field. The addition of the two high-conductivity pathways changed the outline of the plume substantially, although the centre of the mass was nearly the same as for simulation 2 (Fig. 4). The addition of the high-conductivity paths resulted in more dispersion and a more rapid advance of the leading edge of the distribution. Very little of the chemical entered the high conductivity regions and the non-sorbing chemical largely passed between the two regions with low conductivity as with simulation 2. The combination of the high-conductivity and low-conductivity regions created a divided plume at the leading edge, which, on the basis of field sampling, could possibly be identified as two plumes.

With simulation 4 (Fig. 6), the consequences of disturbing the symmetry of the hydraulic-conductivity field were considered. The configuration of the hydraulic conductivity field for simulation 4 was changed by eliminating one of the high-con-

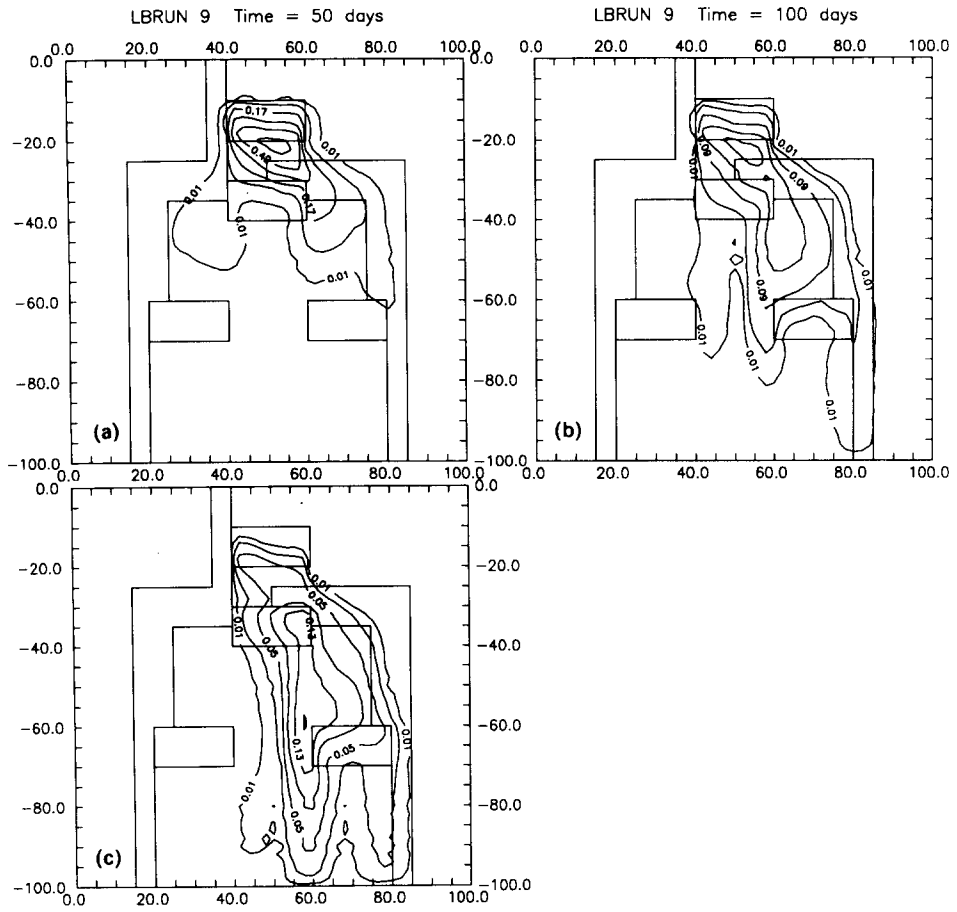

Fig. 8. Simulation 6. Distribution of non-sorbing chemical, initially present in the source area defined by (40, 10; 60, 10; 60, 20; 40, 20), after 50, 100 and 150 days of simulated transport, shown in frames labelled (a), (b) and (c), respectively. Hydraulic conductivity field as shown in diagram, with one high-conductivity path connecting inflow and outflow boundaries. For this simulation the nodal spacing was 5 m, except at the K field boundaries where nodes were 2.5 m from the boundaries and at the outside boundaries where nodes were 0.1 m from the boundary. Total number of nodes was 1365.

ductivity paths. This change resulted in a plume moving toward the high-conductivity area, in contrast to what happened with simulation 3 (Fig. 5) where the plume did not enter the high-conductivity path. With this simulation, the centre of mass moved further downstream and the non-sorbing chemical was distributed more evenly along the length of the aquifer after 150 days, relative to the previous simulations. The shape of the plume results from the fact that with the configuration of simulation 4, velocities along the centre line of the plume were higher than with simulation 3. Darcy velocity components are provided by LT2VSI but are not shown here.

Contamination often occurs in regions with a fluctuating water table. This occurs, for example, in river deltas where the level of the river fluctuates seasonally. Entry

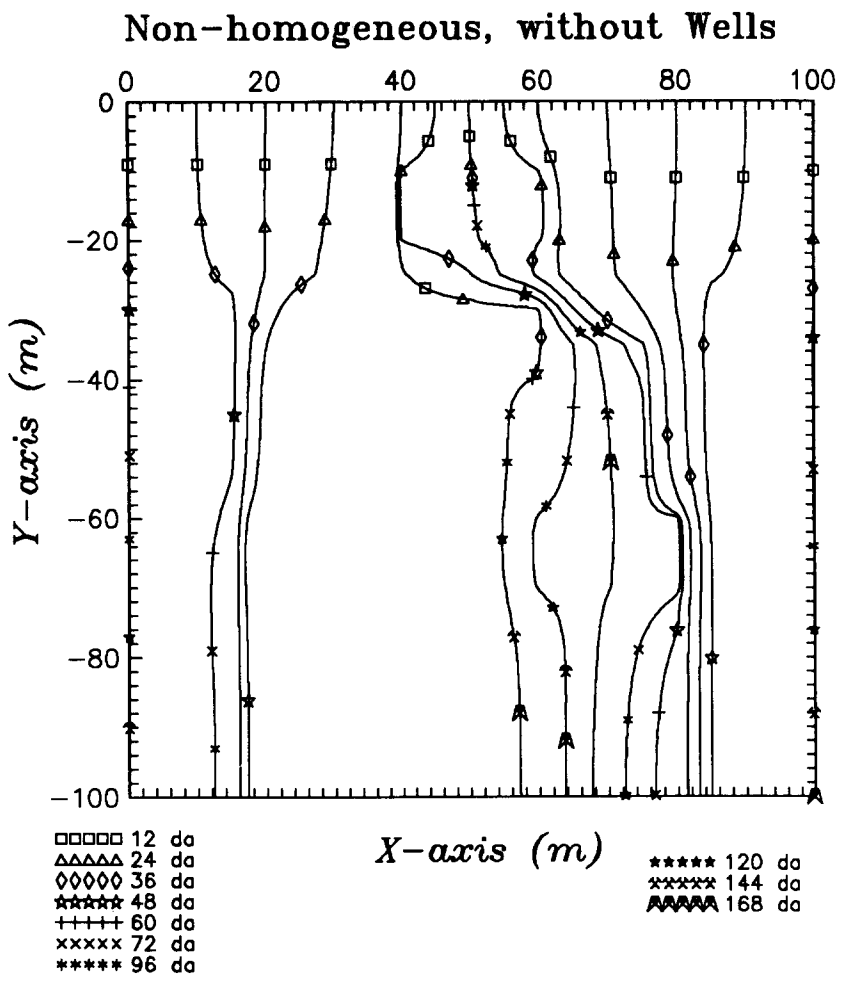

Fig. 9. Flow lines for simulation 6. Each flow line is marked with symbols indicating the distances travelled during the indicated period of time.

into channels of low or high conductivity may depend on water table height so that not all paths are open to the groundwater flow at all times. To evaluate the consequences of changes in availability of channels of high conductivity, the conditions in Fig. 7 were hypothesized for simulation 5. During the first 75 days of simulation, the high-conductivity path was the same as that used for simulation 4 (Fig. 6). During the next 75 days, the high-conductivity path was assumed to be on the left-hand side, instead of on the right-hand side of the flow field when viewed in the direction of flow (Fig. 7c). The resulting distribution shows an increased plume complexity, and at 150 days the plume seems to be breaking up into three parts.

For simulation 6 (Fig. 8), one of the areas of high conductivity was changed to be continuous from the inflow boundary to the outflow boundary. The resulting distribution shows a plume moving away from the high-conductivity path that

Table 2
Highest concentration of the distributions calculated by LT2VSI and shown in Figs. 8, 10 and 11 and relative chemical mass for the same distributions

Simulation and nodal spacing	Number of nodes	Time since start		
		25 days	75 days	150 days
6; spacing 5 m	1365	0.810	0.461	0.160
7; spacing 2 m	5840	0.968	0.594	0.172
8; spacing 1 m	15 125	0.987	0.653	0.270

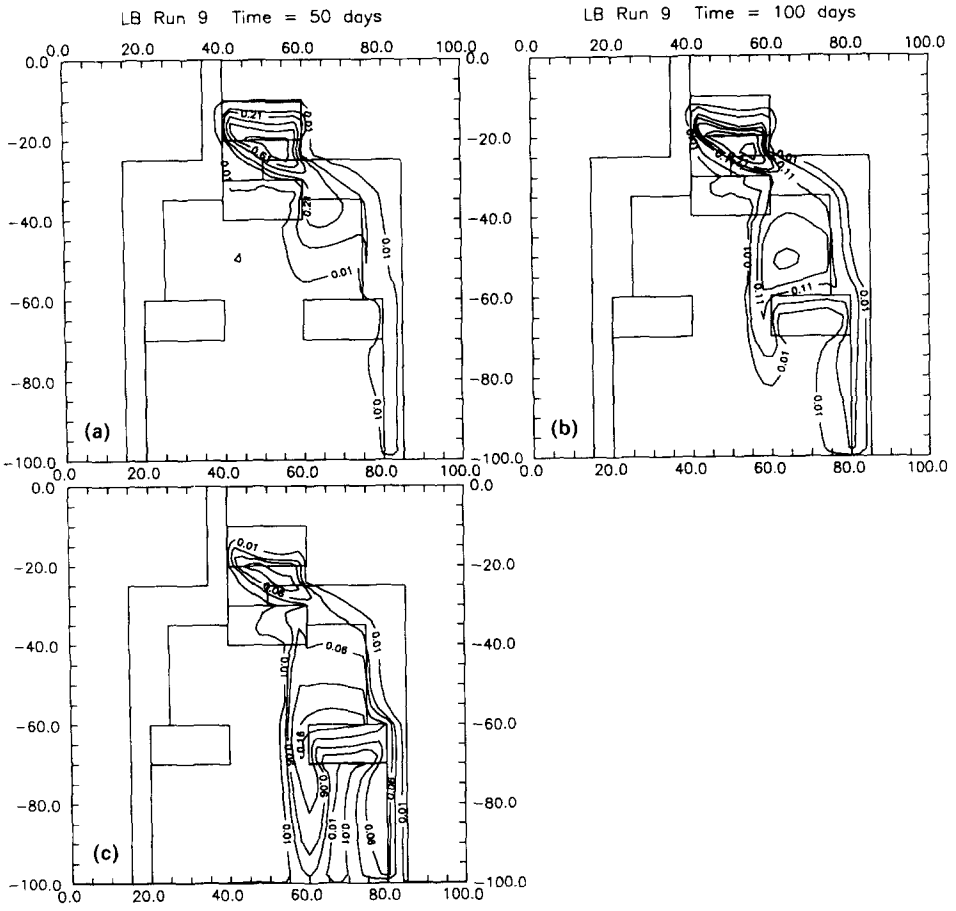

Fig. 10. Simulation 7. Same as simulation 6, but with a nodal spacing of 2 or 5 m throughout the aquifer except at the K field boundaries where nodes were 0.2 m from the boundary and at the outside boundaries where nodes were 0.2 and 0.4 m from the boundary. Total number of nodes was 5840. Distributions are after 50 days (a), 100 days (b) and 150 days (c) of simulated transport.

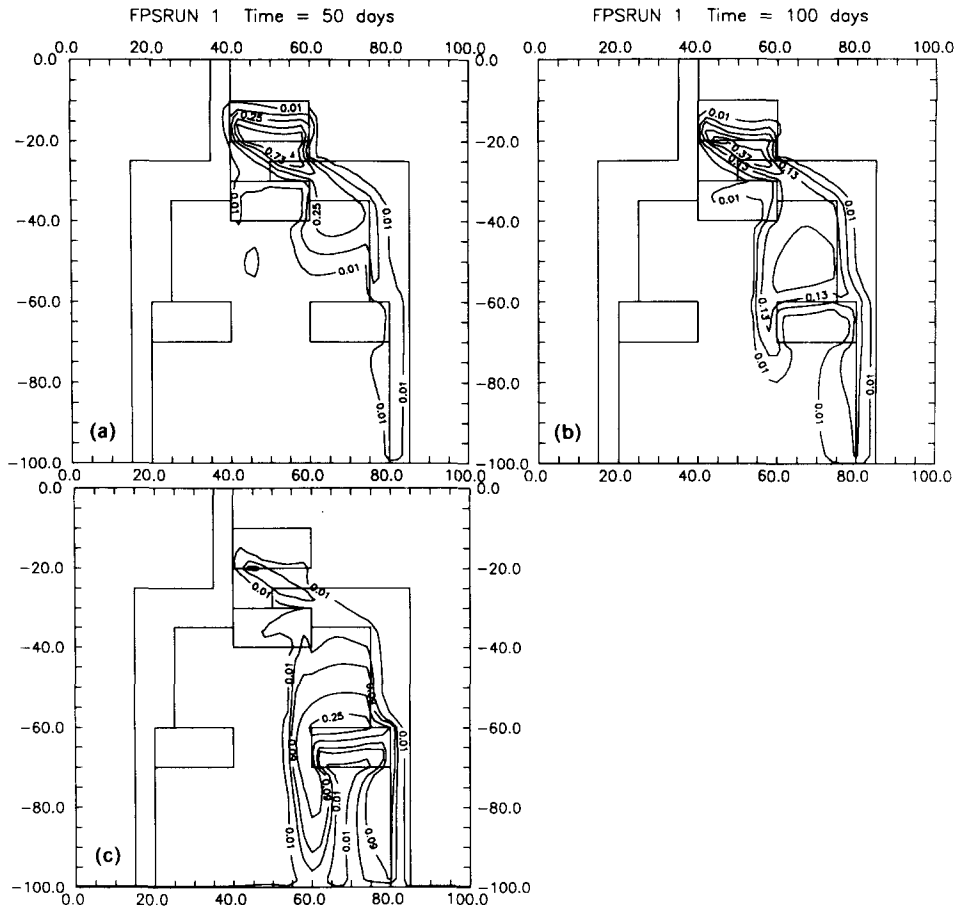

Fig. 11. Simulation 8. Same as simulation 6, but with nodal spacing of 1 m except at the K boundaries, where nodes were 0.1 m from the boundary and at the outside boundaries where nodes were 0.1 and 0.2 m from the boundary. Total number of nodes was 15 125. Distributions are after 50 days (a), 100 days (b) and 150 days (c) of simulated transport.

extended from inflow end to outflow end, but towards the high-conductivity path that originated within the flow field. Flow lines (Fig. 9) corresponding to this geometry resulted from higher pressure in the high-conductivity path, forcing flow away from it.

The effect of nodal spacing on the results of simulation was evaluated using the geometry of simulation 6 (Fig 8). Three simulations were run. The number of nodes were 1365 for simulation 6, 5840 for simulation 7, and 15 125 for simulation 8 (Table 2). For simulation 6, the nodal spacing was 5 m, except that at boundaries, where K changed, the spacing was 2.5 m and, at the outside boundaries, the spacing was 0.1 m. For simulation 7 (Fig. 10) a nodal spacing of 2 m was used with nodes 0.2 m from the boundaries where K changed, and at the outside boundaries the spacings were 0.2 and 0.4 m. With simulation 8 (Fig. 11)

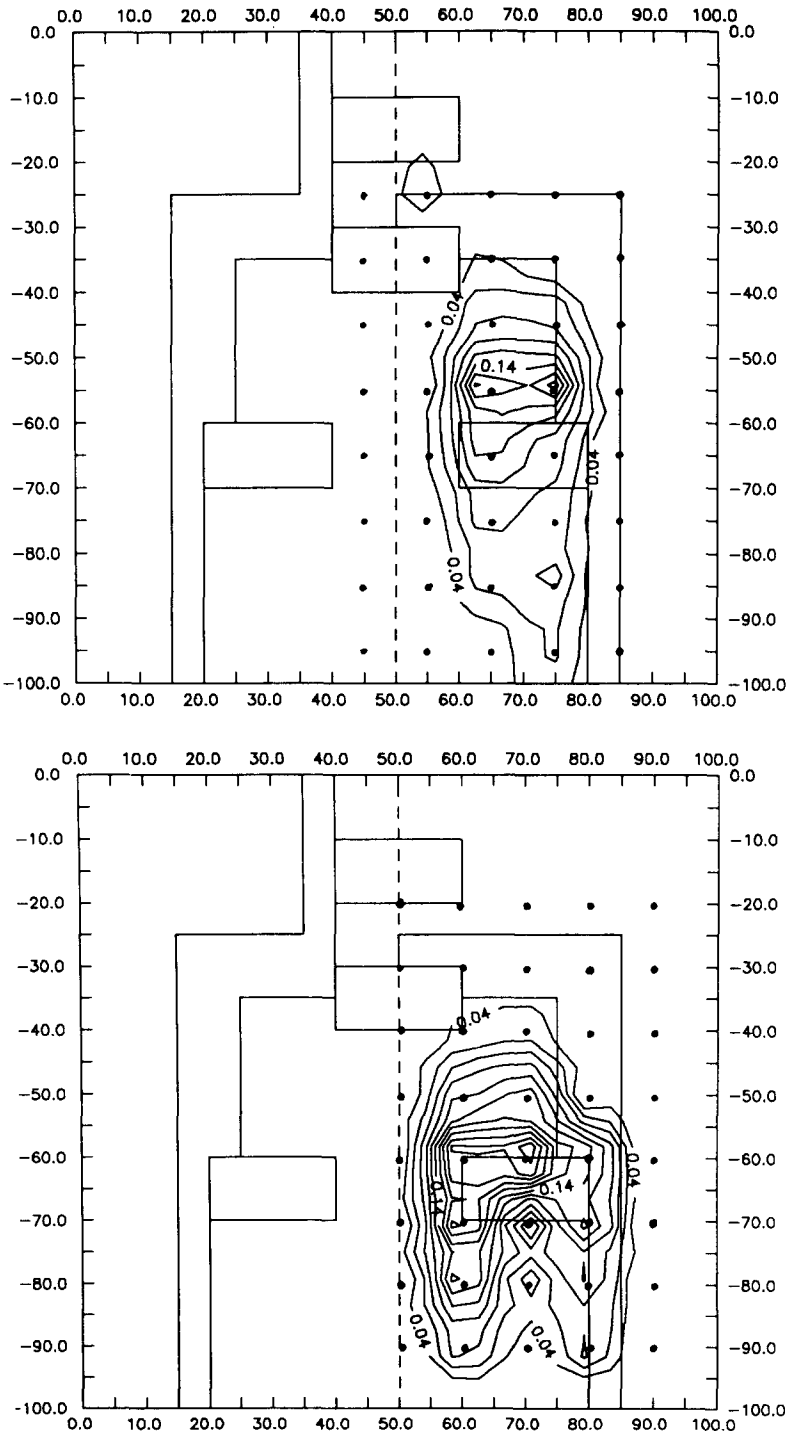
0.0 10.0 20.0 30.0 40.0 50.0 60.0 70.0 80.0 90.0 100.0
0.0
-10.0
-20.0
-30.0
-40.0
-50.0
-60.0
-70.0
-80.0
-90.0
-100.0
0.04
0.14
0.04
0.04
0.04
0.14
0.14
0.04
0.04
0.04

the nodal spacing was 1 m with nodes at 0.1 m on either side of the K boundaries and 0.1 and 0.214 m from outside boundaries. Comparisons between simulations 6, 7, and 8 (Figs. 8, 10 and 11) show the importance of nodal spacing. The highest concentration in the plume for each simulation is shown in Table 2. Numerical dispersion was most pronounced with the largest spacing and increased with length of simulation time and with decreased concentrations (Table 2).

An important aspect of dealing with groundwater quality issues is the identification of the position of the plume. Because sampling is costly, the number of sampling points is usually limited. The question, 'given the complexity of the plume, how important is the choice of sampling locations?' was answered by imposing sampling networks on the distribution for simulation 6 at 150 days (Fig. 8). The sampling points were at 10 m spacings at $x = 44, 54, \ldots, 84$ and $y = 24, 34, \ldots, 94$ for 12A and at $x = 50, \ldots, 90$ and $y = 20, \ldots, 90$ for 12B as shown in Fig. 12. Concentrations at the sampling points were obtained from the computer simulation. The program SURFER was then used to obtain the lines of equal concentration shown in Fig. 12. The sampling network for 12A was chosen so that sampling points were in the high-concentration regions at the leading edge of the plume, but not in the areas of low concentration. For 12B the sampling network was moved over by 6 m so that sampling points also occurred in the areas of low concentration. The mass of chemical for each distribution was determined by integration using Simpson's rule. Setting the concentration of simulation 7 equal to 100, relative concentrations were 85 for 12A, and 125 for 12B. Setting the concentration for 12A equal to 100, the relative concentration for 12B was 68. The choice of sampling grid resulted in substantially different plume geometries and yielded different masses.

4. Conclusions

A two-dimensional transport and fate model for chemicals in a water-saturated sorbing porous medium, e.g. below the water table, was constructed. The model was used to simulate concentration distribution patterns over space and time for aquifers with postulated positional heterogeneities in hydraulic conductivity. These simulations showed the importance of knowledge of the hydraulic conductivity field.

The distribution of a chemical, initially present in a small region of the aquifer, was shown to be affected strongly by the geometry of the hydraulic conductivity field after 150 days of simulated transport, indicating the importance of 'site characterization', i.e. gaining a good working knowledge of the hydraulic conductivity field over space.

Fig. 12. Distribution of chemical obtained by superimposing sampling networks on the distributions of simulations 7 (Fig. 10) and 8 (Fig. 11). The sampling points were at 10 m spacings in the x and y directions at points described in the text. Concentrations at the sampling points were calculated with LT2VSI and lines of equal concentration were drawn using SURFER.

For example, if samples were drawn periodically from a line of sampling wells across a field, an idea of the heterogeneous nature of the aquifer could be obtained if the dispersion terms in the transport and fate model were ignored and the purely advective transport terms were retained, i.e. a particle tracking procedure was used. In the absence of any injection/pumping wells the tracklines are unique and are functions of the intervening hydraulic conductivities. The transit times from the source region to the observation points can be very different for each trackline. Combining the chemical concentrations from each observation point at a given sampling time yields a highly smeared out breakthrough curve which could easily be misinterpreted as coming from a highly dispersive one-dimensional transport and fate process. Yet there is no dispersion in the system at all. Adding the dispersion terms to the model produces an even greater degree of smearing out of the elution curve.

The simulations show the importance of caution in the interpretation of sample data from large-scale heterogeneous aquifers; they emphasize the need to obtain detailed information about the hydraulic conductivity field.

5. References

Alexander, M., 1981. Biodegradation of chemicals of environmental concern. Science, 211: 132–138.

Bear, J. and Verruijt, A., 1987. Modeling Groundwater Flow and Pollution. Reidel, Dordrecht.

Bodvarsson, G., 1984. Linearization techniques and surface operators in the theory of unconfined aquifers. Water Resour. Res., 20: 1271–1276.

Brown, R.A., Norris, R.D. and Brubaker, G.R., 1985. Aquifer restoration with enhanced bioreclamation. Pollut. Eng., 17: 25–28.

Cheng, R.T., Casulli, V. and Milford, S.N., 1984. Eulerian–Lagrangian solution of the convection–dispersion equation in natural coordinates. Water Resour. Res., 20: 944–952.

Dagan, G., 1984. Solute transport in heterogeneous porous formation. J. Fluid Mech., 145: 151–177.

Gelhar, L.W., 1986. Stochastic subsurface hydrology from theory to applications. Water Resour. Res., 22: 135S–145S.

Hess, K.M., Wolf, S.H. and Celia, M.A., 1992. Large-scale natural gradient tracer test in sand and gravel, Cape Cod, Massachusetts. 3. Hydraulic conductivity variability and calculated macrodispersivities. Water Resour. Res., 28: 2011–2027.

Hillel, D. 1980. Fundamentals of Soil Physics. Academic, New York.

Konikow, L.F. and Bredehoeft, J.D., 1978. Computer model of two-dimensional solute transport and dispersion in ground water. In: Techniques of Water-Resources Investigations of the United States Geological Survey, Book 7, Chapter C2. US Dept. Interior, Washington, D.C.

Lee, M.D., Thomas, J.M., Borden, R.C., Bedient, P.B. and Ward, C.H., 1988. Biorestoration of aquifers contaminated with organic compounds. CRC Crit. Rev. Environ. Control, 18: 29–89.

Lehr, J.H. and Nielsen, D.M., 1982. Aquifer restoration and ground water rehabilitation — A light at the end of the tunnel. Ground Water, 20: 650–656.

Lindstrom, F.T. and Boersma, L., 1989. Analytical solutions for convecting–dispersive transport in confined aquifers with different initial and boundary conditions. Water Resour. Res., 25: 241–256.

Lindstrom, F.T., Boersma, L., Barlaz, M. and Beck, F., 1990. Denitrification in nonhomogeneous laboratory scale aquifers. 1. Preliminary model for transport and fate of a single compound. USEPA/600/2-90/

009. USEPA, Env. Research Lab., Ada, Oklahoma.

Lindstrom, F.T., Boersma, L., Myrold, D. and Barlaz, M., 1991. Denitrification in nonhomogeneous laboratory scale aquifers: 4. Hydraulics, nitrogen, chemistry and microbiology in a single layer. USEPA/600/2-91/014. USEPA, Env. Research Lab., Ada, Oklahoma.

Pye, V.I., Patrick, R. and Quarles, J., 1983. Groundwater Contamination in the United States. University of Pennsylvania, Philadelphia.

Van der Hoek, J.P. and Klapwijk, A., 1987. Nitrate removal from ground water. Water Res. 21: 989–997.